Project LaserImplant

D2.1 Images hierarchical spikes and ripples

Reporting period	**from**	**01.01.2021**	**to**	**31.12.2021**
Report completed and released		**23.06.2021** **Jörn Bonse, Martina Muck, Johannes Heitz, Xxx Sedao, Alain Abou Khalil**		

1. Goals

The deliverable **D2.1** provides a collection of SEM images of hierarchical spikes and ripples on cylindrical Ti-based samples published on the **LaserImplant** web-site (www.laserimplant.eu).

2. Detailed Description

Introduction

There are different ways to structure the side walls of cylindrical metal samples with a laser beam – one of the experimental tasks in the **LaserImplant** project. The most simple and straightforward way is scan with a focused laser beam across the cylinder sample. However, for a cylinder radius exceeding the Rayleigh-length of the focused laser beam, this results in a sample, where at maximum the upper half of the cylinder is laser-structured, while the non-transparent metal cylinder itself shades the laser radiation from the lower part of the cylinder. Moreover, in this approach, the angle of incidence of the incident laser radiation locally varies – depending on the lateral position of the laser beam focus on the cylinder wall – and may result in locally varying spatial periods of the laser-induced periodic surface structures (LIPSS, ripples) or orientation of the hierarchical spikes.

BAM

This problem can be overcome by stepwise rotating the cylinder between different laser-processing sequences. Figure 1 provides an example of a Ti6Al4V titanium alloy rod (grade 5, 6 mm diameter) that was polished in first step in order to reduce the sample roughness. In a second step, the polished surface was processed at **BAM** by a focussed Yb-based disk laser beam (wavelength λ = 1030 nm, pulse duration τ = 925 fs, pulse repetition frequency f = 100 kHz, focus diameter $2w_0$ ~ 35 µm, scan velocity v_{scan} = 700 mm/s, line distance ΔS = 5 µm) at a peak fluence F_0 = 0.5 J/cm^2 (lower processed area) and F_0 = 0.6 J/cm^2 (upper processed

area) both with the linear polarization parallel to the cylinder axis. The corresponding laser-processed areas indicate the presence of sub-micrometric LIPSS through their colorized appearance arising from optical diffraction at the grating-like surface ripples.

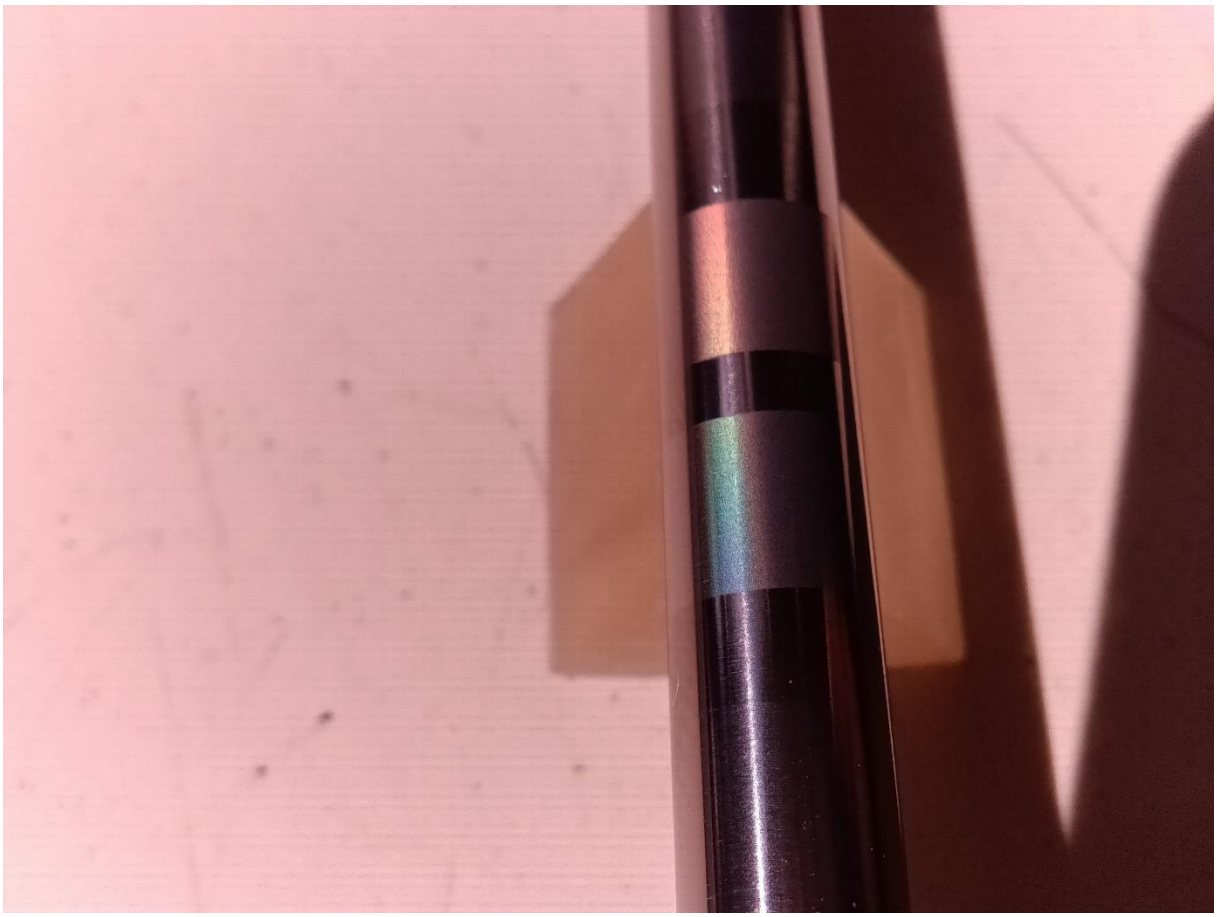

Fig. 1: Photograph of a polished 6-mm diameter Ti6Al4V rod that was laser-processed at two different areas covered by LIPSS (ripples) featuring spatial periods of ~800 nm. The color shade arises from optical diffraction of the illuminating natural sun-light at the surface ripple structures.

For visualizing the ripples in the lower area processed at F_0 = 0.5 J/cm^2, high-resolution optical microscopy was employed in dark-field illumination mode using a long working distance 100× microscope objective. For overcoming the problem of the very limited depth-of-focus in high-resolution microscopic imaging (~1 µm for the given condition), a series of differently focused micrographs (“z-stack”) was acquired and used to process a high-resolution optical micrograph of extended depth of focus, see Fig. 2.

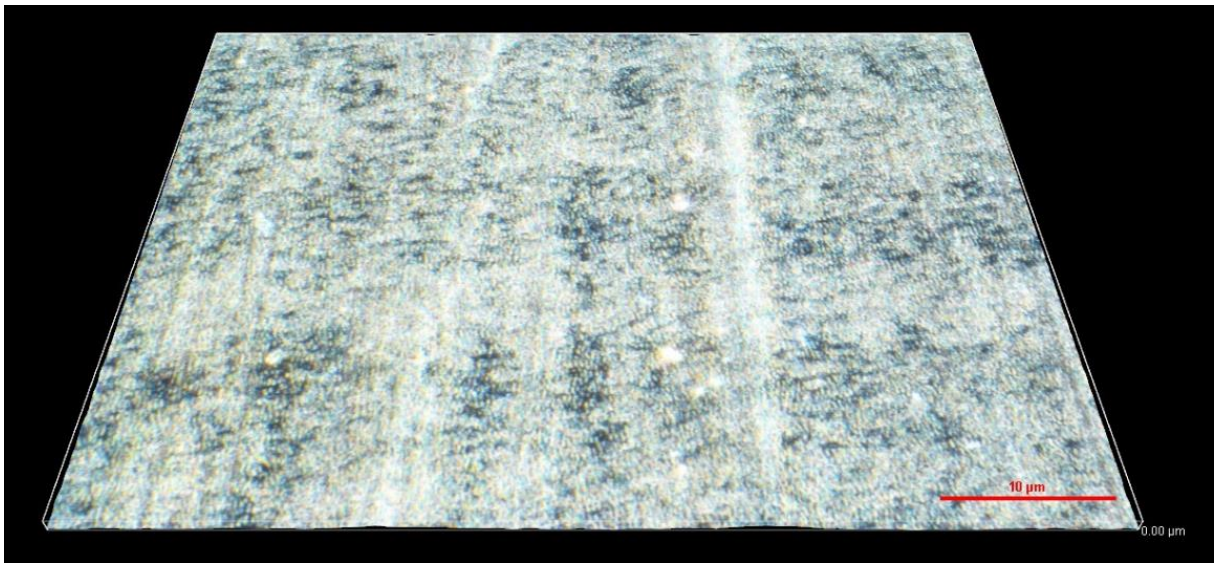

Fig. 2: 3D-view of a z-stacked series of high-resolution optical micrographs of a laser-processed Ti-rod surface previously shown in Fig. 1 featuring LIPSS (vertical) that are oriented perpendicular to the laser beam polarization. The cylinder axis is horizontal. The curvature of the cylinder surface can be recognized at the left/right borders of the bounding box.

Although already close to the optical diffraction limit of the optical microscope, the (nano)ripples are clearly resolved as vertical line pattern, while also the cylinder surface curvature becomes visible at the left/right borders of the bounding box in Fig. 2.

JKU

For the images in this deliverable **D2.1**, **JKU** uses a Yb-based femtosecond laser set-up (Spirit 1040-16 HE, Spectra Physics, wavelength λ = 1040 nm, pulse duration τ = 350 fs) to produce a laser beam that is guided through a system of five mirrors and focused by a lens (100 mm focus length) onto the sample stage, which can be moved linearly in two dimensions. The diameter of the focused laser beam is $2w_0$ = 50 µm ± 2 µm. To be able to produce conical structures with superimposed nanoripples (LIPSS), a parameter set (peak fluence F_0, scanning velocity v_{scan} and line distance ΔS) is determined beforehand based on parameters such as laser type (wavelength and pulse duration), focused beam diameter $2w_0$ and the desired laser frequency f.

For cylindrical Ti-based samples, a continuous rotation during laser structuring was chosen, which was investigated only on titanium cylinders of 8 mm diameter until now, but can be adapted to other cylindrical samples such as bone screws and dental implants. A schematic of the spiral approach for area structuring on cylindrical sample is shown in Fig. 3. While rotating, the sample is moved along the y-axis with a velocity v_{scan} that leads to the desired line distance ΔS. Pulse repetition rate f and y-axis velocity can be chosen according to the desired rotation speed.

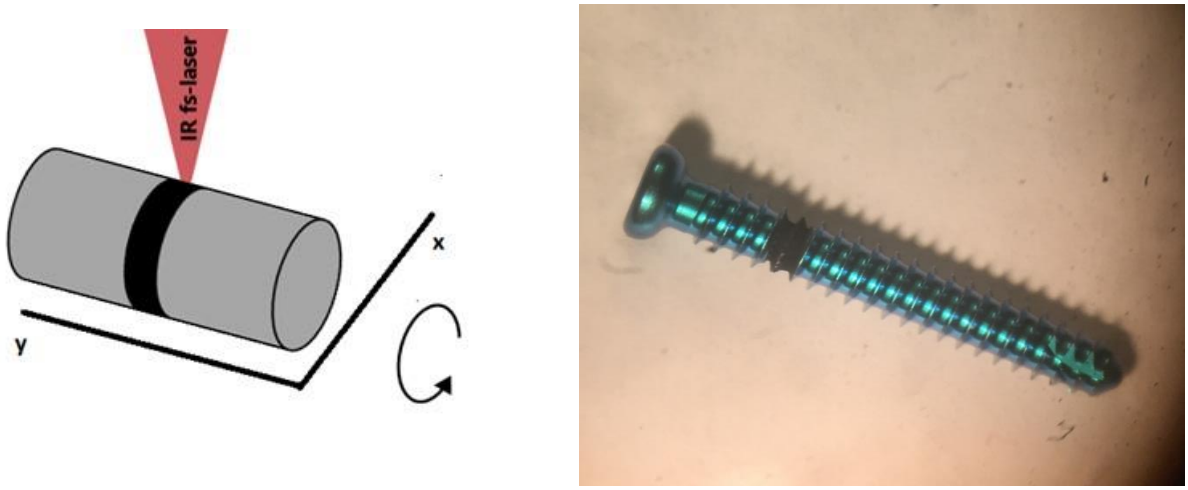

Fig. 3: The left image shows the schematics of continuous laser processing of cylindrical samples. The laser is focused onto the highest point of the cylindrical sample. For continuous laser processing, the sample is irradiated while being rotated and moved along the *y*-axis, leading to a spiral around the cylinder. The right image shows a bone-screw (length 17 mm, diameter 2.5 mm) with a laser-processed ring in black (the blue color of the screw results from the pre-anodization). Figure adapted from [1].

For testing, a rotation speed of 2500 ms/round trip was chosen. Several tests revealed the necessity of a pulse repetition rate f = 33 kHz and a peak fluence F_0 = 4.3 J/cm^2 to produce conical microstructures with superimposed nanoripples. For continuously structuring the sample, a velocity v_{scan} = 6 µm/s along the *y*-axis was chosen to achieve areas with laser line distances of ΔS = 15 µm. Scanning electron microscopy (SEM) images of aforementioned ring on a titanium cylinder are shown in the following Figs. 4 and 5.

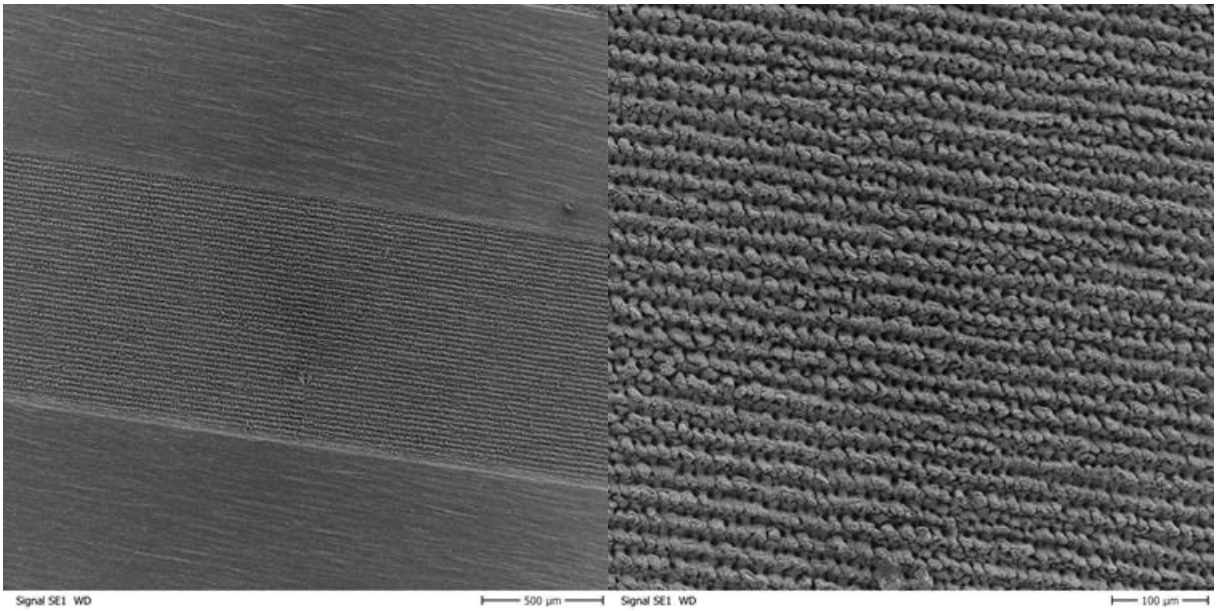

Fig. 4: Overview SEM image of a ring produced by ultrafast laser structuring in a spiral approach (left). Close-up of ring with densely-packed spike microstructures (right).

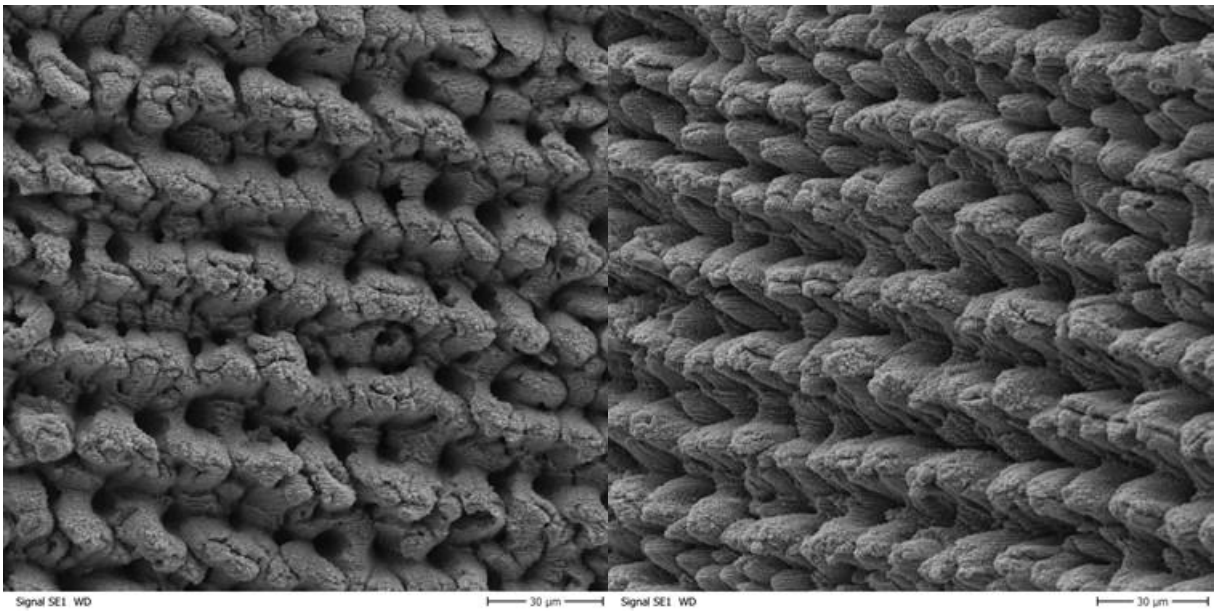

Fig. 5: Magnified view SEM images of spike microstructures with superimposed nanoripples (left). Corresponding side view of the hierarchical micro-/nanostructures on cylindrical sample (right).

Additionally to cylinders, also pre-anodized Ti-based bone screws (from the product line of **HOFER**) were processed line-by-line (with many pulses per area) with the Yb-based femtosecond laser of **JKU**. Figure 6 shows SEM images of a 1 mm wide ring with peak fluence $F_0 \approx 2.6$ J/cm^2, writing speed of 350 µm/s, a line-to-line distance of 30 µm, and a pulse repetition rate $f = 1$ kHz. More details can be found in Ref. [1].

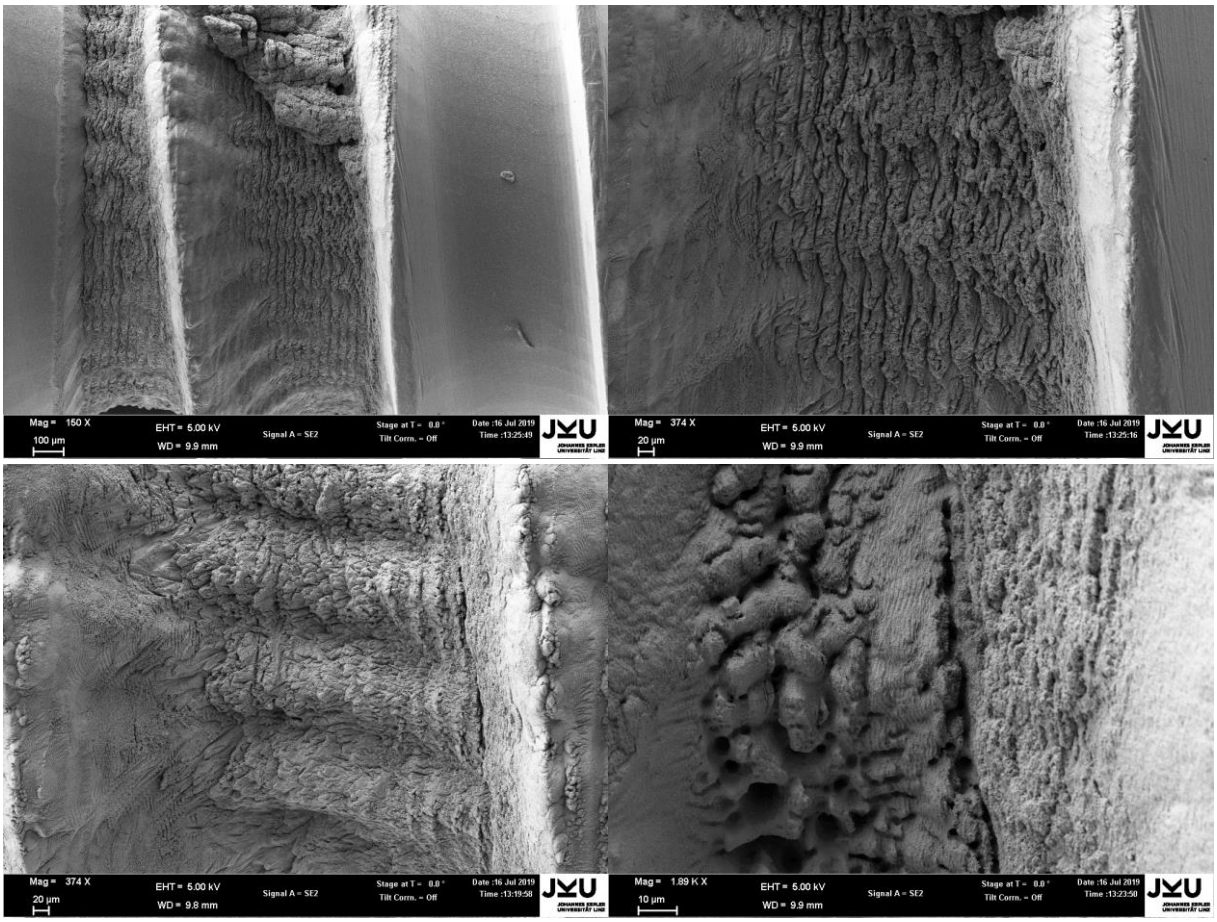

Fig. 6: SEM images of magnified spike microstructures with superimposed nanoripples on a laser-processed ring on a bone screw. The screw is covered by inhomogeneous structures, as the windings of the screw partially block the laser surface irradiation.

UJM

As a part of the preliminary trials, **UJM** tested a bone screw (from **HOFER**) patterning strategy of using a Bessel beam. As shown in the low magnification optical microscope image in Fig. 7, the laser beam in Bessel configuration scanned along the rotational axis of the bone screw. Two zones of single-line scans are highlighted by the yellow boxes in this image. A small selected area in one of the boxes is further magnified and shown in the optical microscope image on the right.

The initiative of deploying of Bessel beam is due to the fact that a Bessel beam has a greater distance/volume along its propagation direction, within which a homogeneous laser patterning can be realized. It is thought that Bessel beam patterning of the cylindrical surface of the bone screw body and the windings has an advantage of being less sensitive to these surface topography variations. If a third of the screw surface could be Bessel beam patterned homogeneously by raster scanning the Bessel beam in this part of the screw, the whole screw would be fully texturized by a combined action consisting of raster scanning and step rotation of 120 degree along its rotational axis after each scan. For upscaling and process acceleration, this strategy has a potential merit.

The ultrafast laser irradiation of **HOFER** bone screws was carried out using a Ti:Sapphire laser system (of model Legend from Coherent Inc.) at 1 kHz and a central wavelength 800 nm, pulse duration 100 fs in this case. The Bessel beam was generated by an axicon with a = 5°, and de-magnified through a 4f-telescopic afocal arrangement (lens 1: *F1* = 100 mm and lens 2: *F2* = 75 mm). The resulted beam has a conical half-angle θ = 3°, a diameter of central core $2w_b$ = 11 mm, and a Bessel beam length z_b = 43 mm. The laser power was set at 467 mW (hence 467 µJ/pulse). These conditions determined that the laser fluence was approximately at F_0 = 1.5 J/cm^2 at the central core part of the Bessel beam (detailed calculation of Bessel fluence can be found in Ref. [2]). The scan speed was varied between v_{scan} = 500 µm/s and 1 mm/s.

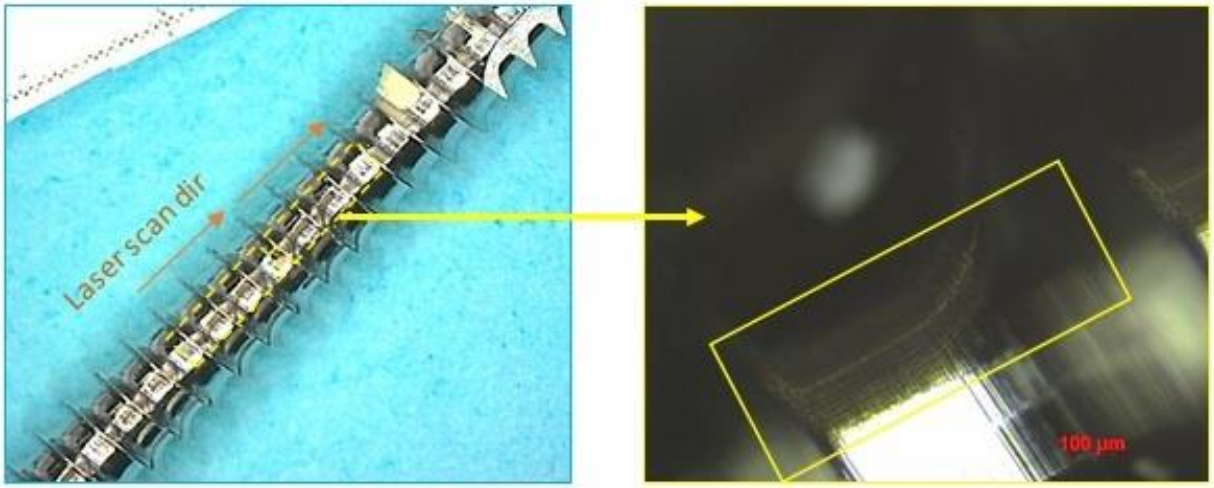

Fig. 7: Optical microscope images of **HOFER** bone screw partially textured using a Bessel beam setup. The low magnification view (left) is showing the positions of the laser-patterned areas on the screw. The higher magnification image (right) is showing a localized area within the valley between two windings.

Due to the limitations of the depth of the field, as well as the distance between the microscope objective and the screw, details of the laser patterning are not resolved by the optical analysis. Therefore, SEM inspection was necessary. For this, a couple of SEM micrographs are presented in Fig. 8. The SEM micrograph on the left revealing the cylindrical body part of the screw with one thread/winding separating two adjacent valleys. The inset is a rotated optical microscope image for visual guidance that indicates the position of the screw in SEM. A small area of interest is further studied at higher a magnification, as is shown in Fig. 8 (right). Ripples of LSFL-type are seen to cover the laser irradiated track. Aside from the ripples, there is also an additional surface undulation at approximately 10 µm interval. This undulation is thought to be part of the initial surface topography of the screw but not related to laser irradiation. Three laser scan tracks of same laser condition were produced each time on the surface of the screw and they were 0.5 mm apart (2 of the 3 are visible in Fig. 8, left micrograph). Due to the cylindrical surface topography of the screw, these tracks were at different distances to the laser source. Nonetheless the presence of the ripples has been confirmed in all the tracks.

The more interesting areas to investigate would be laser-irradiated ones on the winding surface. Unfortunately, the screws were rather cumbersome in the SEM chamber and advanced positioning such as tilt was not possible. Nevertheless, the present results suggest further study should be encouraged. Smaller samples (sectioned screws for instance) should be prepared for the ease of post-mortem observation, and large area raster scanning might be a better choice for patterning homogeneity investigation.

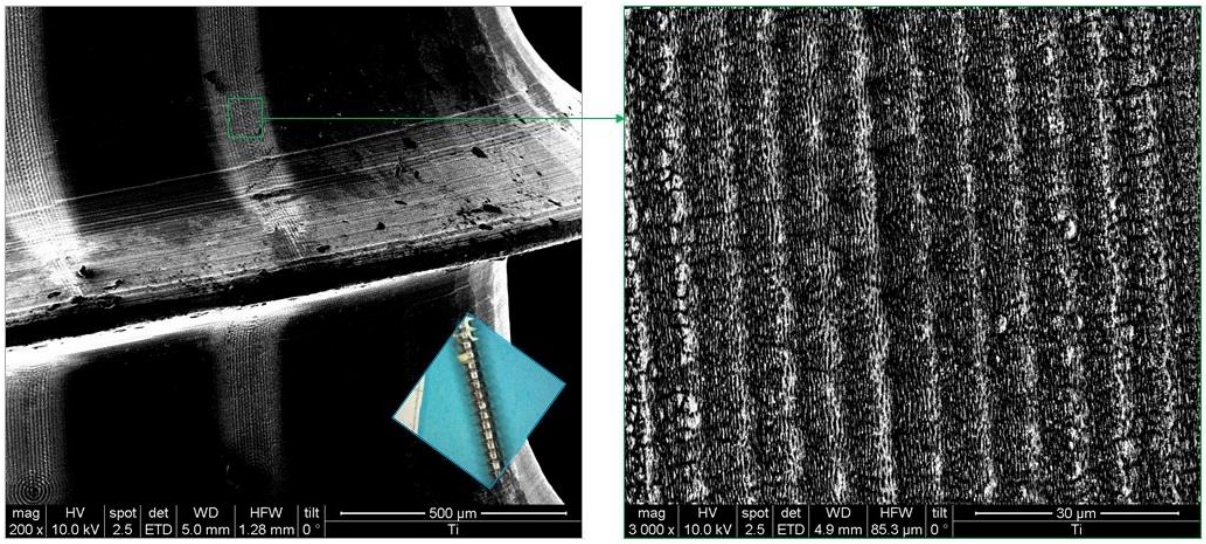

Fig. 8: Magnified view SEM images of two bands of laser scanned areas (left), the inset indicates the positioning of the screw in SEM chamber. Enlarged view of a selected zone from the SEM image on the left (right).

References

[1] M. Muck, B. Wolfsjäger, K. Seibert, C. Maier, S. Ali Lone, A.W. Hassel, W. Baumgartner, J. Heitz: *„Femtosecond Laser-Processing of Pre-Anodized Ti-Based Bone Implants for Cell-Repellent Functionalization“*, Nanomaterials **11** (2021), 1342.
https://doi.org/10.3390/nano11051342

[2] H.D. Nguyen, X. Sedao, C. Mauclair, G. Bidron, N. Faure, E. Moreno, J.-P. Colombier, R. Stoian: *"Non-Diffractive Bessel Beams for Ultrafast Laser Scanning Platform and Proof-Of-Concept Side-Wall Polishing of Additively Manufactured Parts"*, Micromachines **11** (2020), 974. https://doi.org/10.3390/mi11110974

Both articles [1,2] are Open Access Publications published under the Creative Commons Attribution license CC-BY 4.0.

3. Evaluation of Goals and Resulting Actions

The deliverable **D2.1 Images hierarchical spikes and ripples** was finalized in time by m6. A link to this report was implemented into the Dissemination the **LaserImplant** web-site (www.laserimplant.eu). A screenshot is shown below.

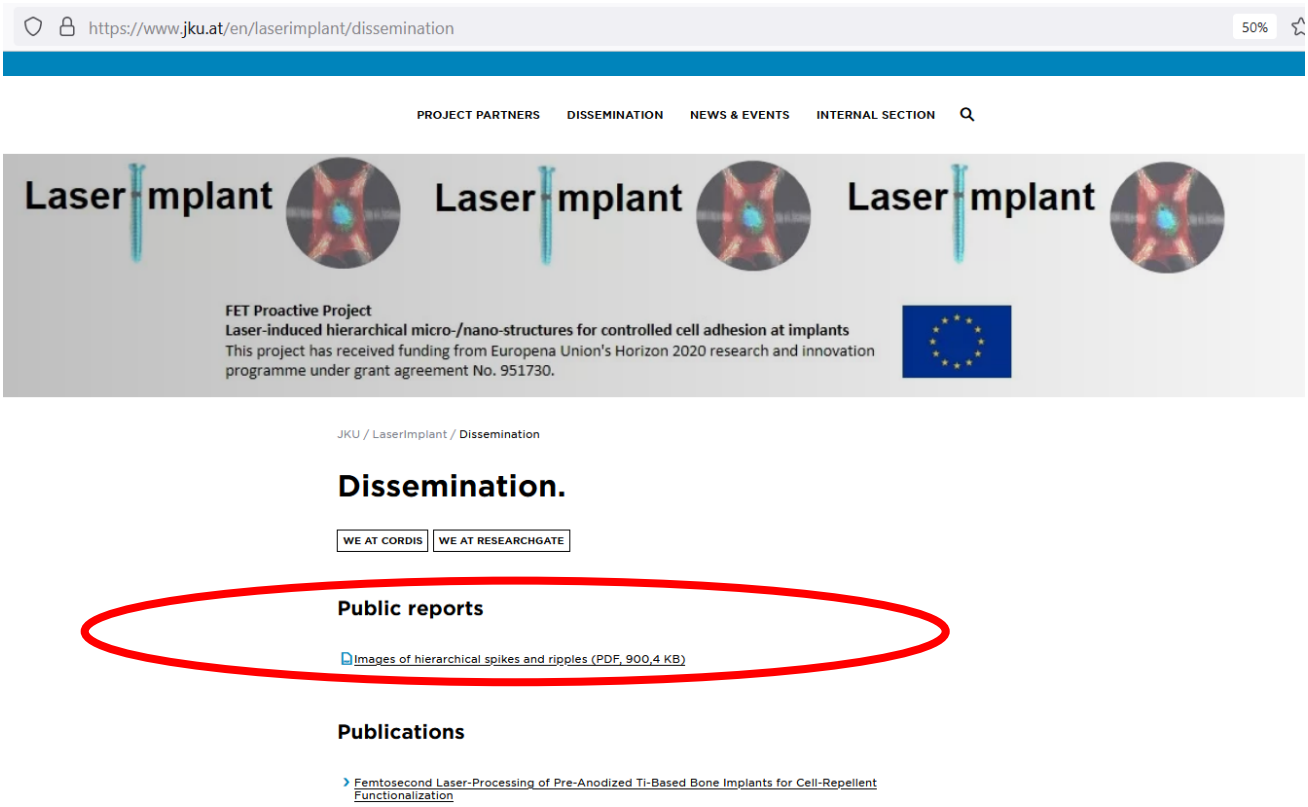

Fig. 9: Screenshot of the Dissemination section of **LaserImplant** web-site taken on June 23, 2021.